J. King Saud Univ., Vol. 18, *Eng. Sci*. (1), pp. 139-160, Riyadh (1426H./2005)

Gravity Gradient Effect on a LEO Satellite with an Elliptic Orbit and Unsymmetrical Mass Properties

K. Alsaif* and K. Al-Dakkan**

** Mechanical Engineering Department, King Saud University, Riyadh, Saudi Arabia and Space Research Institute, King Adbdulaziz City for Science and Technology, Saudi Arabia*

*** Space Research Institute, King Adbdulaziz City for Science and Technology, Saudi Arabia*

(Received 15 March, 2005; accepted for publication 03 July, 2005)

Abstract. The study presented in this paper investigates the dynamic behavior of a low earth orbit (LEO) satellite due to gravity gradient disturbances when the product of inertia terms of the spacecraft and the orbit eccentricity are considered. It is shown that the classical stable solution for the gravity gradient disturbance becomes unstable if at least one product of inertia term exceeds a critical value. Dimensional analysis technique is used to develop the significant dimensionless groups which were used to correlate the data generated from the response of the coupled roll, pitch and yaw dynamics. Based on the findings of these groups, stability maps are developed to predict the influence of the product of inertia terms on the long-term behavior of the spacecraft attitude dynamics. The developed stability maps are verified numerically and successful prediction of a spacecraft stability condition due to gravity gradient disturbance is achieved.

Nomenclature

r	*distance from the center of inertial coordinated X,Y,Z to an element of mass dm*
θ_i	*rotation about i direction, i = x,y, or z*
ω_i	*angular velocity component , i = x,y, or z*
$\dot{\omega}_i$	*angular acceleration component , i = x,y, or z*
e	*orbit eccentricity*
a	*semi-major axis*
I_i	*mass moment of inertia about the body axes i (x,y, or z)*
I_{tot}	$I_x+I_y+I_z$
I_{ij}	*product of inertia, i and j = x,y, or z*
G	*Newton's constant of gravitation*
m	*mass of satellite*
l_{ir}	*directional cosine , i = x, y, or z and r denotes radial direction*
$\vec{H}$	*angular momentum vector*
f	*true anomaly*

Introduction

The influence of the gravitational torques on satellite dynamics and stability has been treated intensively in the literature. However, the majority of the treatments considered in this area focused on spacecrafts with special shape and mass properties. For instance, Chen [1] combined the gravity gradient torque and aerodynamic torque in order to reach three axes stabilization. The analysis was based on a circular orbit and the cross products of inertia (off diagonal elements of the inertia tensor) were assumed to be zero. Ravindran [2] performed active control analysis based on gravity gradient and aerodynamic torques assuming a circular orbit and no variation in the moment of inertia of the satellite.

Zanardi [3] made a comparison between two satellites to show the effect of the gravity gradient, solar radiation, aerodynamic and magnetic torques at specific altitude in a circular orbit and the cross product of moments of inertia were ignored. The analysis illustrates that gravity gradient torque is very sensitive to the geometry and dimensions of the satellite.

Roach [4] referred to the failure of their implementation of three-axis gravity gradient stabilization on ATS-2 satellite due to improper modeling of the gravity gradient disturbance as well as the neglected orbit eccentricity factor. Frik [5] investigated the stability of a rigid body satellite in a circular orbit in the presence of aerodynamic and gravitational torques when both have the same order of magnitude. He concluded that lack of stability exists if non-conservative aerodynamic torques exist. Flanagan [6], shed more lights on passively stabilized spacecraft using Liapunov stability theory with the assumption of principle coordinates. Ashneberg [7] and Shrivastava [8] analyzed the effect of elliptical orbit on the dynamics of the satellite and concluded that in the existence of elliptical orbit, the system could experience periodic excitation in yaw, row or pitch depending on the geometry of the spacecraft.

Therefore, the current study investigates the influence of the products of inertia magnitude and orbit eccentricity on the attitude response and stability of a satellite (for a passive mode i.e. without actuators) due to gravity gradient moments. To generalize the results, dimensional analysis technique is used to develop significant groups (groups which are formed by combination of the system parameters i.e. I_{xz} , I_x , etc.) which will contribute to the development of stability maps to aid in predicting the long-term dynamic behavior of the system. These maps can be utilized during the preliminary design stage of the spacecraft to investigate its passive instability behavior (due to gravity gradient disturbance) for a given set of product of inertia terms.

It is noted that some satellite control engineers in the development stage of the control algorithms neglect the product of inertia terms when modeling the gravity gradient torques acting on the satellite. In some cases, where the pitch and roll inertias are very close, errors can be introduced in the modeling of the gravity gradient torque if

the product of inertia effects are ignored.

Gravity Gradient Torque on an Orbiting Rigid Body

The gravitational force acting on an element of mass "*dm*" , as shown in Fig. 1-a, of a rigid body orbiting a spherically symmetrical primary body is given by;

$$d\vec{F} = \frac{\mu}{r^3}(\vec{r}_c + \vec{\rho})dm$$

where ; $\mu = G\,m$

$\vec{r}_c$ position vector to the mass center of the rigid body and can be expressed as;

$$\vec{r}_c = r_c\,(l_{xr}\,i + l_{yr}\,j + l_{zr}\,k)$$

$\vec{\rho}$ locates the element of mass *dm* relative to the satellite mass center which can be written as;

$$\vec{\rho}\ \ \vec{\rho} = x\,i + y\,j + z\,k$$

The moment of the gravity force $d\vec{F}$ about the mass center *c* is given by:

$$d\vec{M}_c = -\frac{\mu}{r^3}\ \ (\vec{\rho}\times\vec{r}_c)dm$$

Integrating over the entire body; the total gravity gradient torque can be expressed as;

$$\vec{M}_c = -\mu \int_m \frac{(\vec{\rho}\times\vec{r}_c)dm}{r^3} \qquad \text{(1-A)}$$

In order to evaluate this integral, r^3 must be written in terms of $\vec{r}_c$ and $\vec{\rho}$.
According to the law of cosine

$$r^2 = \rho^2 + r_c^2 + 2\vec{\rho}\cdot\vec{r}_c \quad \text{or}$$

$$r^2 = r_c^2 \cdot \left(1 + \frac{2\vec{\rho}.\vec{r}_c}{r_c^2} + \left(\frac{\rho}{r_c}\right)^2\right)$$

for small $\frac{\rho}{r_c}$, the term $\left(\frac{\rho}{r_c}\right)^2 \approx 0$

using the binomial expansion for the remaining terms yields;

$$\frac{1}{r^3} \approx \frac{1}{r^3{}_c}\left(1 - \frac{3(\vec{\rho}.\vec{r}_c)}{r_c^{\,2}}\right) \qquad \left|\frac{\rho}{r_c}\right| \langle\langle\ 1 \qquad \text{(1-B)}$$

Substituting equation (1-b) into (1-a) and expressing the vectors $\vec{r}_c$ and $\vec{\rho}$ in the body axes as defined above, the integral can be expanded as follows

$$\begin{aligned} \mathrm{r}\\ \mathrm{M_c} &= -\frac{\mu}{\mathrm{r_c^{\,2}}}\int_{\mathrm{m}}\left(1-\frac{3(\mathrm{x\,l_{xr}+y\,l_{yr}+z\,l_{zr}})}{\mathrm{rc}}\right)\\ &\times\left\{\left(\mathrm{y\,l_{zr}-z\,l_{yr}}\right)\mathrm{i}+\left(\mathrm{z\,l_{xr}-x\,l_{zr}}\right)\mathrm{j}+\left(\mathrm{x\,l_{yr}-y\,l_{zr}}\right)\mathrm{k}\right\}\mathrm{dm} \end{aligned} \qquad (2)$$

for small angle approximations ($\cos(\theta) \approx 1,\ \sin(\theta) \approx \theta$), the direction cosines can be expressed as;

$$l_{xr} = 1, \qquad l_{yr} = -\theta_z \text{ , and } \qquad l_{zr} = \theta_y \qquad (3)$$

substituting equation (3) into (2) and evaluating the integral, the gravity gradient torque about each of the body axes can be expressed as follows (note: $\int xdm = \int ydm = \int zdm = 0$);

$$\begin{aligned} M_x &= \frac{3\mu}{r_c^3}\left(I_{xy}\theta_y + I_{xz}\theta_z\right)\\ M_y &= \frac{3\mu}{r_c^3}\left(\left(I_x - I_z\right)\theta_y - I_{yz}\theta_z + I_{xz}\right)\\ M_z &= \frac{3\mu}{r_c^3}\left(\left(I_x - I_y\right)\theta_z - I_{yz}\theta_y - I_{xy}\right) \end{aligned} \qquad (4)$$

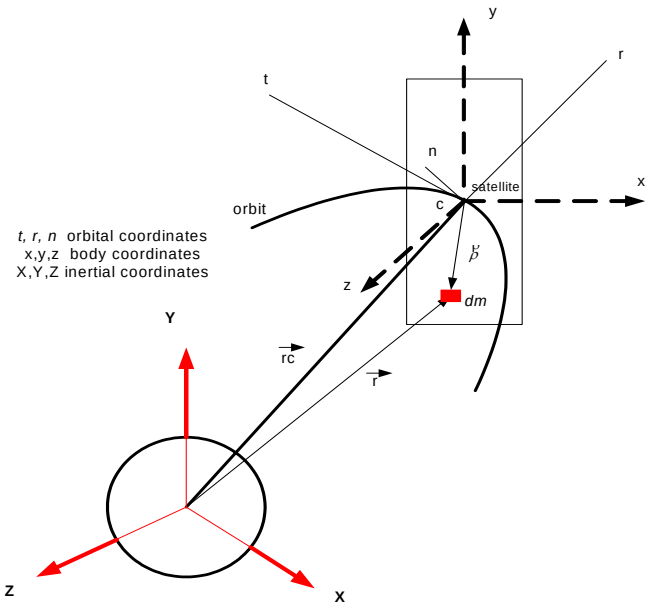

Fig. 1-a. Satellite in orbit a round the earth (system geometry and coordinates).

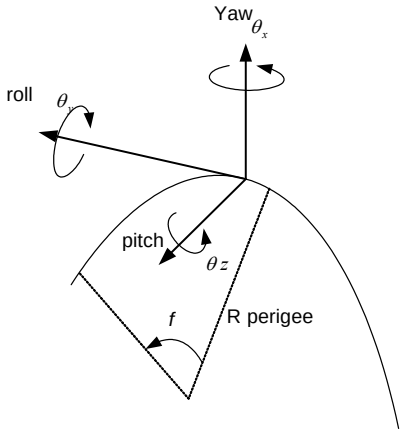

Fig. 1-b. Angles definition – (note: body coordinates aligned with orbital coordinates).

System Formulation

Consider a rigid satellite with coordinates system illustrated in Fig. 1-a. If the axes origin is selected as the body center of mass, the rotational equations of motion can be written as ;

$$\vec{M}_c = \dot{\vec{H}}_c = \dot{H}_x i + \dot{H}_y j + \dot{H}_z k + \vec{\omega} \times \vec{H}_c \tag{5}$$

or in component form along the body axes;

$$\begin{aligned}
M_x &= I_x \dot{\omega}_x + \omega_y \omega_z \left(I_z - I_y\right) + I_{xy}\left(\omega_x \omega_z - \dot{\omega}_y\right) - I_{xz}\left(\omega_x \omega_y + \dot{\omega}_z\right) - I_{yz}\left(\omega_y^2 - \omega_z^2\right) \\
M_y &= I_y \dot{\omega}_y + \omega_z \omega_x \left(I_x - I_z\right) + I_{yz}\left(\omega_x \omega_y - \dot{\omega}_z\right) - I_{xy}\left(\omega_y \omega_z + \dot{\omega}_x\right) - I_{xz}\left(\omega_z^2 - \omega_x^2\right) \\
M_z &= I_z \dot{\omega}_z + \omega_x \omega_y \left(I_y - I_x\right) + I_{xz}\left(\omega_y \omega_z - \dot{\omega}_x\right) - I_{yz}\left(\omega_z \omega_x + \dot{\omega}_y\right) - I_{xy}\left(\omega_x^2 - \omega_y^2\right)
\end{aligned} \tag{6}$$

defining θ_x , θ_y and θ_z as shown in Fig. 1-b and using the rotation sequence (θ_y , θ_z , θ_x), the component of the angular velocity vector, in body coordinates, can be expressed as;

$$\begin{Bmatrix} \omega_x \\ \omega_y \\ \omega_z \end{Bmatrix} = [R_1(\theta_x)][R_3(\theta_z)][R_2(\theta_y)] \begin{Bmatrix} 0 \\ 0 \\ \dot{f} \end{Bmatrix} + [R_1(\theta_x)][R_3(\theta_z)] \begin{Bmatrix} 0 \\ \dot{\theta}_y \\ 0 \end{Bmatrix} + [R_1(\theta_x)] \begin{Bmatrix} 0 \\ 0 \\ \dot{\theta}_z \end{Bmatrix} + \begin{Bmatrix} \dot{\theta}_x \\ 0 \\ 0 \end{Bmatrix} \tag{7}$$

where

$$\dot{f} = \frac{n\left(1 + e\ \ Cos(f)\right)^2}{\left(1 - e^2\right)^{3/2}} \qquad \text{from reference [9]}$$

$$R_1(\theta_x) = \begin{bmatrix} 1 & 0 & 0 \\ 0 & \cos(\theta_x) & \sin(\theta_x) \\ 0 & -\sin(\theta_x) & \cos(\theta_x) \end{bmatrix}, \quad R_2(\theta_y) = \begin{bmatrix} \cos(\theta_y) & 0 & -\sin(\theta_y) \\ 0 & 1 & 0 \\ \sin(\theta_y) & 0 & \cos(\theta_y) \end{bmatrix}, \text{ and } \quad R_3(\theta_z) = \begin{bmatrix} \cos(\theta_z) & \sin(\theta_z) & 0 \\ -\sin(\theta_z) & \cos(\theta_z) & 0 \\ 0 & 0 & 1 \end{bmatrix}$$

for small angles approximation, Eq. (7) can be simplified to;

$$\begin{Bmatrix} \omega_x \\ \omega_y \\ \omega_z \end{Bmatrix} \approx \begin{Bmatrix} \dot{\theta}_x - \theta_y n \\ \dot{\theta}_y + \theta_x n \\ \dot{f} + \dot{\theta}_z \end{Bmatrix} \tag{8}$$

and the angular acceleration vector as,

$$\begin{Bmatrix} \dot{\omega}_x \\ \dot{\omega}_y \\ \dot{\omega}_z \end{Bmatrix} \approx \begin{Bmatrix} \ddot{\theta}_x - \dot{\theta}_y n \\ \ddot{\theta}_y + \dot{\theta}_x n \\ \ddot{\theta}_z \end{Bmatrix} \tag{9}$$

where $n = \sqrt{\frac{Gm}{a^3}}$

Considering only the gravity gradient disturbance (for linear system the other disturbances like the solar and magnetic moments can be added separately) and substituting Eqs. (4), (8) and (9) into Eq. (6) yields the following equations of motion,

$$\begin{aligned}
&I_x\ddot{\theta}_x - I_x n\dot{\theta}_y + (I_z - I_y)n\dot{\theta}_x + (I_z - I_y)n^2\theta_y + I_{xy}n^2\theta_x - I_{xy}n\dot{\theta}_y - I_{xy}n\dot{\theta}_x - I_{xy}\ddot{\theta}_y - I_{xz}n^2 \\
&-I_{xz}\ddot{\theta}_z + I_{yz}n^2 + 2I_{yz}n\dot{\theta}_z - 3n_s^2\left(I_{xy}\theta_y + I_{xz}\theta_z\right) = 0 \\
&I_y\ddot{\theta}_y + I_y n\dot{\theta}_x + (I_x - I_z)n\dot{\theta}_x - (I_x - I_z)n^2\theta_y - I_{yz}\ddot{\theta}_z - I_{yz}n^2 - I_{xy}n\dot{\theta}_x - I_{xy}n\dot{\theta}_y - I_{xy}\ddot{\theta}_x + nI_{xy}\dot{\theta}_y \\
&-I_{xz}n^2 - 2I_{xz}n\dot{\theta}_z - 3n_s^2\left(I_x - I_z\right)\theta_y + 3n_s^2 I_{yz}\theta_z - 3n_s^2 I_{xz} = 0 \\
&I_z\ddot{\theta}_z + I_z n^2 + I_{xz}n\dot{\theta}_y + I_{xz}n^2\theta_x - I_{xz}\ddot{\theta}_x + I_{xz}n\dot{\theta}_y - I_{yz}n\dot{\theta}_x + I_{yz}n^2\theta_y - I_{yz}n\dot{\theta}_x - I_{yz}\ddot{\theta}_y \\
&-3n_s^2\left(I_x - I_y\right)\theta_z + 3n_s^2 I_{xy} + 3n_s^2 I_{yz}\theta_y = 0
\end{aligned} \tag{10}$$

where , $n_s = \sqrt{\frac{Gm}{r_c^3}}$

Numerical Solution and Results

The equations of motion presented in (10) are strongly coupled linear time varying differential equations. The equations consider only the effect of eccentricity and gravity gradient torques as environmental disturbances. The equations contain all three product of inertia terms. It should be noted that stability analysis using analytical approach is outside the scope of this study and would be considered for publication separately.

A Simulink model is developed, to integrate the equations of motion and obtain the time history of the roll, pitch and yaw. There are 5 cases considered in this study as follows;

1- $Ixz = Ixy = Iyz = 0$ (in this case x,y, and z are principle coordinates)

2- $Ixz \neq 0$, $Ixy = Iyz = 0$

3- $Iyz \neq 0$, $Ixy = Ixz = 0$

4- $Ixy \neq 0$, $Ixz = Iyz = 0$

5- $Ixz \neq 0$, $Ixy \neq 0$, $Iyz \neq 0$

in all cases, the eccentricity is varied from 0 to 0.3. In the first case , it can be shown analytically; Kaplan [9], that the attitude of the satellite(subjected to gravity gradient torque only) in circular orbit is stable in roll, yaw and pitch if;

$I_z > I_y > I_x$ *or* $I_y > I_x > I_z$ (all product of inertia terms are zero) (11)

In the other cases, where at least one product of inertia term is present, the solution may undergo instability even though the stability condition (11) is satisfied. The instability definition considered in this study is based on unbounded oscillations (slowly or fast growing response) of the satellite attitude. In other words, a solution with bounded oscillations within the small angles assupmtion is considered stable.

Table 1 summarizes the numerical values for the inertial properties of a satellite selected as case study. It should be noted that the inertia values I_x,I_y and I_z, listed in the table satisfy the criteria indicated in (11). The table includes the corresponding critical values of the product of inertia I_{xz} and I_{yz} that renders the attitude response unstable. Values of product of inertia below the critical limit would keep the system stable. It should be noted that, in practical designs, the magnitude of the product of inertia terms is kept minimum. However, quantifying this minimum for stable attitude dynamics is considered the aim of this study.

Intensive numerical experiments, for different inertia parameters and eccentricity values, have been conducted and only a sample results is summarized and listed in Table 2.

It was observed that the increase of orbit eccentricity would increase the amplitude of attitude oscillations as shown in Figs. 2 and 3, and the system response will be unstable if the spacecraft mass properties satisfy the relation;

$$\frac{I_y - I_x}{I_z} \approx \frac{1}{3}$$ (pitch resonance condition)

Reference [9] shows the derivation of this condition.

It was also noticeable from the substantial amount of data generated from the numerical solution that by increasing the product of inertia terms beyond a critical value the attitude response will grow unstable as shown in Figs. 4 to 6. Figure 4 depicts the attitude response of the satellite with I_{xz} = 0.1 Kg/m^2, $I_{yz} = I_{xy} = 0$; the response is stable in roll, pitch and yaw. Figure 5 shows the unstable response when the value of the product of inertia I_{xz} was increased to 15 kg/m^2.

Furthermore, if at least two product of inertia terms are present (i.e. I_{xz} and I_{yz}) in the equations of motion, the solution will be unstable and the response grows fast for higher product of inertia values. Obviously, it will take longer time for the satellite response to diverge if very small product of inertia terms exist. If $I_{yz} = I_{xz} = 0$, and $I_{xy} \neq 0$, the attitude response is always stable in pitch and unstable in roll and yaw as shown in Figs. 6-a and 6-b. By noting that the expression for the rate of change of the true anomaly is time varying, it can be readily seen from the equations of motion that parametric excitations (i.e. terms like $\dot{f}\dot{\phi}$) are the main source of instabilities and contribute significantly to the unstable behavior of the system for a given set of product of inertias. It can be shown analytically that for $\dot{f} = 0$, the solution is stable provided that the condtion of equation (11) is satisfied.

Table 1. Numerical values of the inertia parameters , Kg m^2

I_x	I_y	I_z	I_{xz} (critical) X	I_{yz} (critical) X
30	75	130	10	65
35	75	130	10.2	60
40	75	130	10.3	55
45	75	130	10.4	50
50	75	130	10.5	44
55	75	130	11.5	38
60	75	130	12.5	32
65	75	130	14.5	25
50	70	130	15	39
50	75	130	10.5	44
50	80	130	6	48
50	75	110	0.5	24
50	75	115	2.5	40
50	75	120	5	41
50	75	125	8	43
50	75	130	10.5	44

Table 2. Numerical experiments results

Figure #	System parameters	Response
Figure 2	$e=0$, $I_{xy} = I_{yz} = I_{xz} = 0$	Attitude is stable in roll, yaw and pitch
Figure 3	$e=0.2$, $I_{xy} = I_{yz} = I_{xz} = 0$	Stable solution, higher amplitude in pitch
Figure 4	$e=0.1$ $I_{xz}/I_{tot} = 1/255$ $I_{xy} = I_{yz} = 0$	Stable, beat response in pitch with high amplitude
Figure 5	$e=0.1$ $I_{xz}/I_{tot} = 15/255$ $I_{xy} = I_{yz} = 0$	Unstable solution in pitch, roll and yaw.
Figure 6	$e=0.1$ $I_{xy}/I_{tot} = 15/255$ $I_{xz} = I_{yz} = 0$	Stable in pitch, unstable in yaw and roll
Figure 7	$e=0.1$ $I_{xy}/I_{tot} = 0.5/255$, $I_{yz}/I_{tot} = 0.7/255$, $I_{xz}/I_{tot} = 0.6/255$	Unstable in all attitude angles

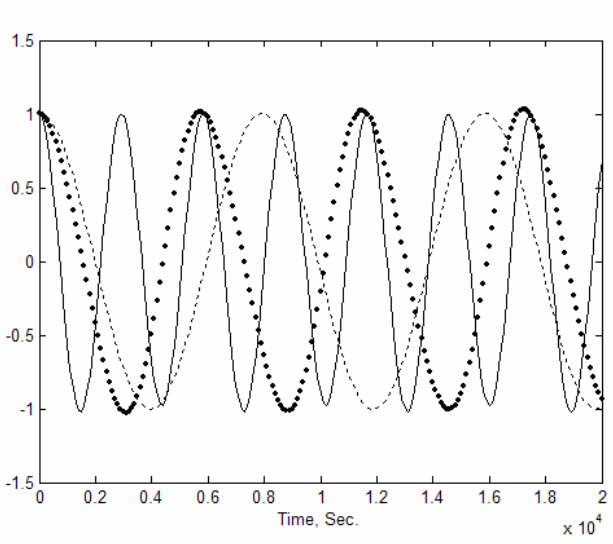

Fig. 2. Attitude response of the satellite in degrees, $I_{xy}=I_{xz}=I_{yz}=0$, $I_x=50$, $I_y=75$, $I_z=135$, e = 0, yaw……, roll _____ , pitch - - - - - - -.

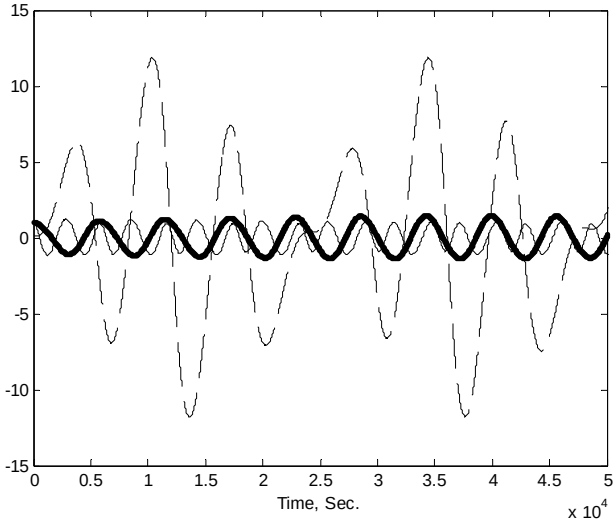

Fig. 3. Attitude response of the satellite in degrees, $I_{xy} = I_{xz} = I_{yz} = 0$, e = 0.2, yaw …… , roll _____ , pitch - - - - - - -.

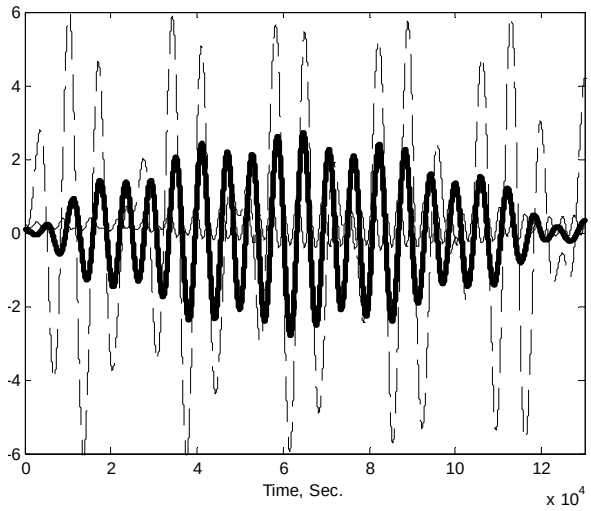

Fig. 4. Attitude response of the satellite in degrees, e = 0.1 and I_{xz}/I_{tot} =1/255. yaw …… , roll _____ , pitch - - - - - - -.

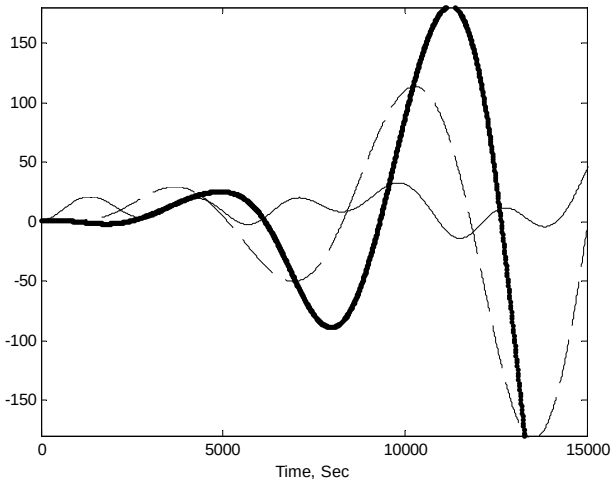

Fig. 5. Attitude response of the satellite in degrees, e = 0.1 and I_{xz}/I_{tot} = 15/255. yaw …… , roll _____ , pitch - - - - - -.

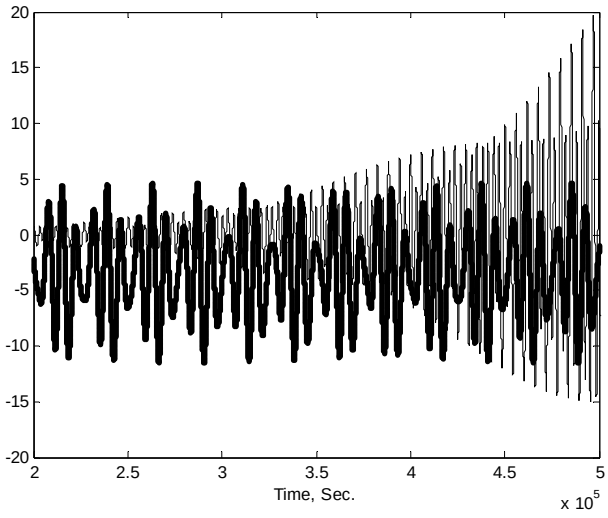

Fig. 6-a. Roll-pitch response in degrees, e = 0.1 and I_{xy}/I_{tot} =15/255 (stable pitch and unstable roll).

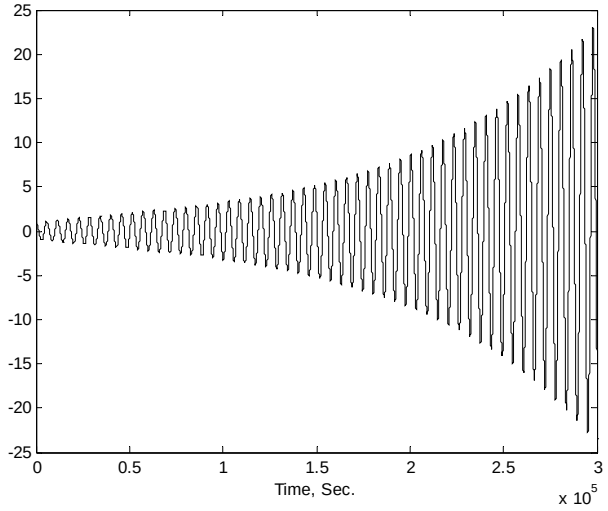

Fig. 6-b. Yaw response in degrees, e = 0.1, I_{xy}/I_{tot}=15/255.

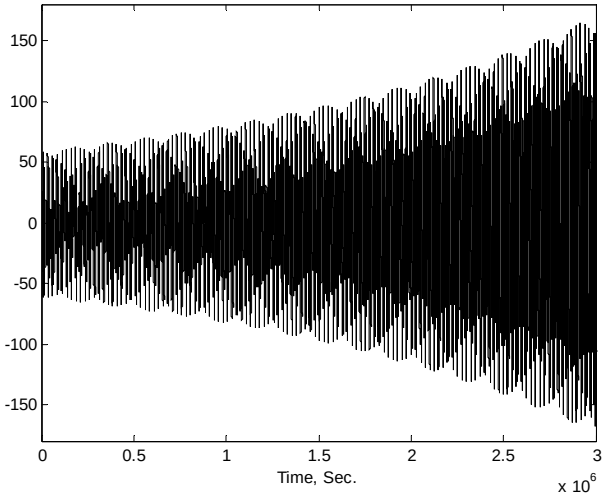

Fig. 7. Pitch response in degrees, e = 0.1 , I_{xy}/I_{tot}= 0.5/255, I_{yz}/I_{tot}= 0.6/255, I_{xz}/I_{tot} = 0.7/255.

After intensive numerical experiments of the normalized equations of motion and collecting substantial amount of data which was processed according to the dimensional analysis techniques (i.e. the detailed of which is not presented); the following significant dimensionless groups are obtained;

$$D_1 = \frac{I_{xz}}{I_x + I_y + I_z} \tag{12}$$

$$D_2 = \frac{I_{yz}}{I_x + I_y + I_z} \tag{13}$$

$$D_3 = \frac{I_x + I_y + I_z}{I_x} \tag{14}$$

$$K_1 = \frac{I_z - I_y}{I_x} \quad , \quad K_2 = \frac{I_z - I_x}{I_y}, \quad K_3 = \frac{I_y - I_x}{I_z} \qquad \text{(by definition)} \tag{15}$$

$$K_{eq} = \sqrt{K_1^{\,2} + K_2^{\,2} + K_3^{\,2}} \tag{16}$$

theses groups are obtained according to the following procedure;

1) define the basic dimensionless parameters of the system (i.e. $\frac{I_{xz}}{I_{tot}}$, $\frac{I_{yz}}{I_{tot}}$, etc.).
2) normalize the equations of motion and obtain the potential significant dimensionless groups.
3) plot each group against the fundamental group, in this case D_1 and D_2 , and calculate the correlation coefficient of the relationship. If the coefficient is close to one then the selected groups can be considered significant.
4) make intensive numerical runs of the equations of motion and use the significant dimensionless groups to present the data in 2D plot. If all data points lie along a specific relationship with error less than 5% , then the developed groups can be used to predict the dynamic behavior of the system as well be shown next.

Now plotting $\frac{K_{eq}}{D_3}$ and K_3 versus D_1 and D_2 , respectively; Figs. 8 and 9 show, approximately, a straight line correlation between the proposed dimensionless groups. All data points obtained from the numerical experiments follow the trend line shown in the figures with a good correlation. The line indicates the border between stable and unstable solutions. It should be noted that the border line points represent a stable solution below which instabilities manifest. The upper region represents the unstable solution in roll, yaw and pitch and the lower region represents the stable solution. The stability charts shown in Figs. 8 and 9 can be used to predict the stability of the satellite attitude due to gravity gradient torques with the presence of product of inertia parameters I_{xz} and I_{yz}, respectively. For the case of I_{xy}, any non-zero value of which would render the system stable in pitch, and unstable in roll and yaw as shown in Fig. 7.

These stability maps are tested intensively and verified with numerical solution of the equations of motion and a sample results is summarized in Table 3. For instance, the first case in the table represents a satellite with a value of .045 for I_{xz}/I_{tot} , $I_{xy} = I_{yz} = 0$, I_{tot} =220 kg m^2 and 0.3662 for K_{eq}/D_3 ,from the stability chart in Fig. 8 the solution is predicted to be stable. To confirm this prediction, the numerical solution for this case is shown in Fig. 10, which shows a bounded solution in pitch, roll and yaw. Similarly, the dynamic response shown in Figs. 11 to 17 confirms the remaining cases listed in the table. It should be noted that numerous experiments, to test the prediction results based on the stability maps proposed, have been conducted with successful results and no single case has proven otherwise. These charts can be utilized during the development stage of the spacecraft to investigate its passive insatiability behavior for a given set of product of inertia terms.

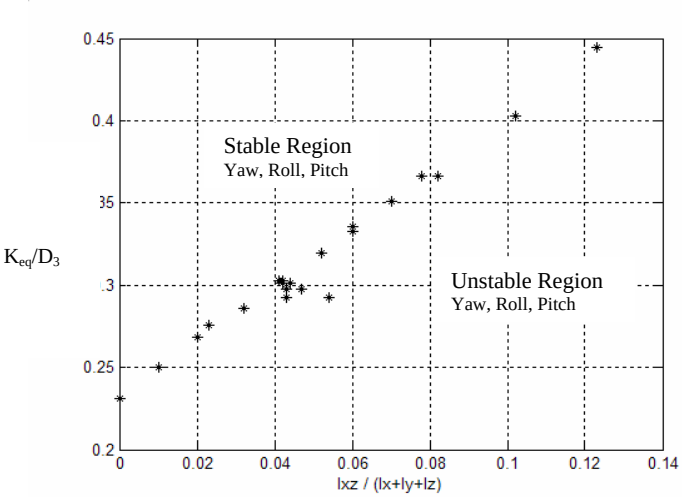

Fig. 8. Gravity gradient–stable and unstable regions as a function of I_{xz} (I_{xy}=I_{zy}=0).

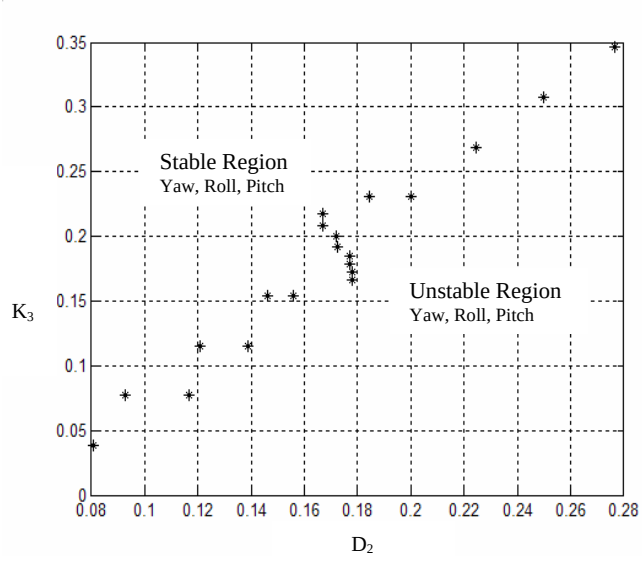

Fig. 9. Gravity gradient–stable and unstable regions as a function of I_{yz} (I_{xy} = I_{zx} = 0).

Table 3. Verification of the developed stability charts in figures (8),and (9) [stable : S , Unstable : U], $I_{xy} = 0$

I_x , I_y ,I_z	I_{xz}/I_{tot}	I_{yz}/I_{tot}	K_{eq}/D_3	K_3	Chart Fig. 8	Chart Fig. 9	Confirm with numerical solution
40,60,120	10/220 = .045	0	0.3662	-	S	-	S, Figure 10
40,60,120	20/220 = .09	0	0.3662	-	U	-	U, Figure 11
15,20,45	5/80 = .0625	0	0.4209	-	S	-	S, Figure 12
15,20,45	10/80 = .125	0	0.4209	-	U	-	U, Figure 13
40,60,120	0	10/220	-	0.167	-	S	S, Figure 14
40,60,120	0	20/220	-	0.167	-	U	U, Figure 15
10,20,30	0	7/60	-	0.333	-	S	S, Figure 16
10,20,30	0	17/60	-	0.333	-	U	U, Figure 17

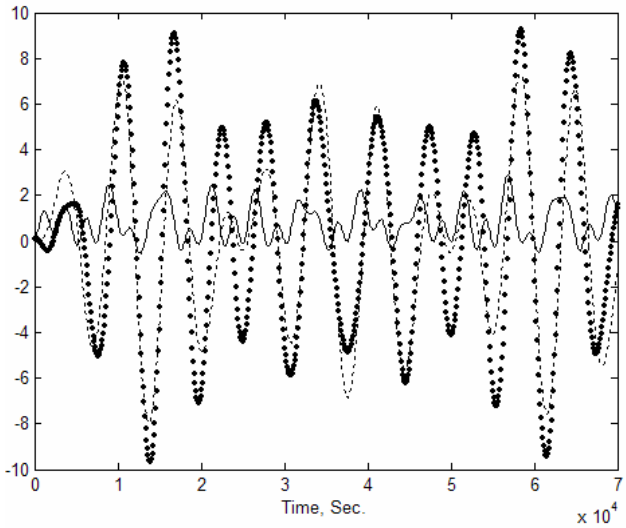

Fig. 10. Attiude response of the satellite in degrees , e = 0.1, I_x = 40, I_y = 60, I_z = 120. and I_{xz}/I_{tot} = 10/220. yaw …… , roll _____ , pitch - - - - - - -.

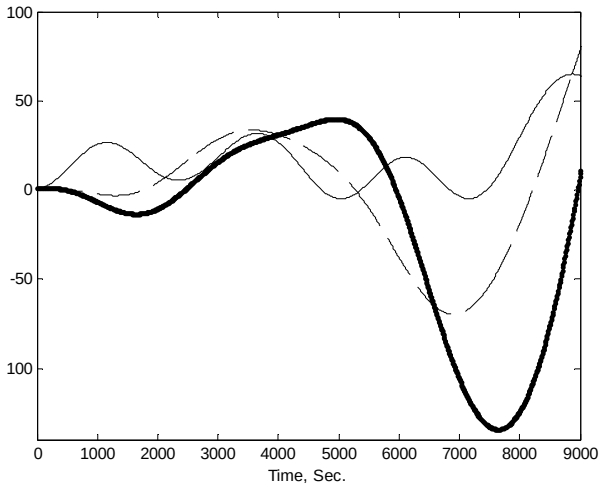

Fig. 11. Attitude response of the satellite in degrees, e = 0.1, I_x= 40, I_y = 60, I_z = 120 and I_{xz}/I_{tot} = 20/220. yaw …… , roll _____ , pitch - - - - - - -.

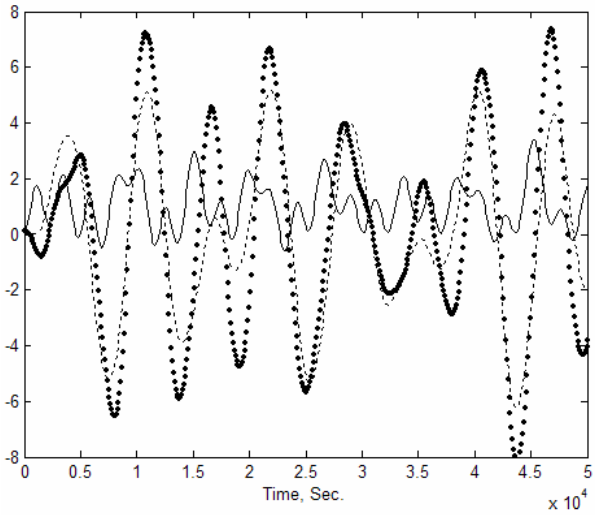

Fig. 12. Attitude response of the satellite in degrees, e = 0.1, I_x = 15, I_y=20, I_z = 45 and I_{xz}/I_{tot} = 5/80. yaw …… , roll _____ , pitch - - - - - - -.

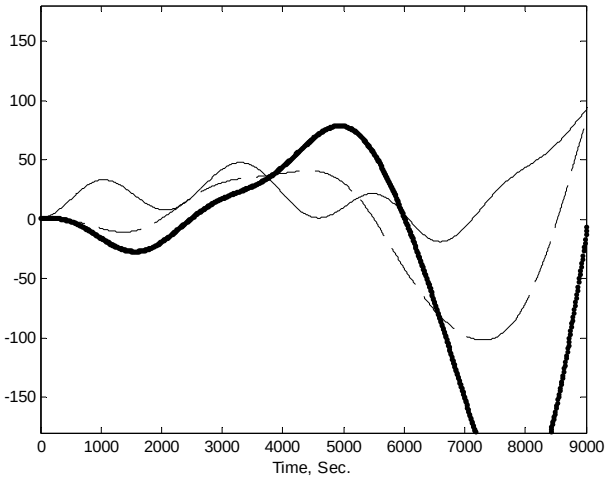

Fig. 13. Attitude response in degrees, e = 0.1, I_x = 15, I_y = 20, I_z = 45 and I_{xz}/I_{tot} = 10/80. yaw …… , roll _____ , pitch - - - - - - -.

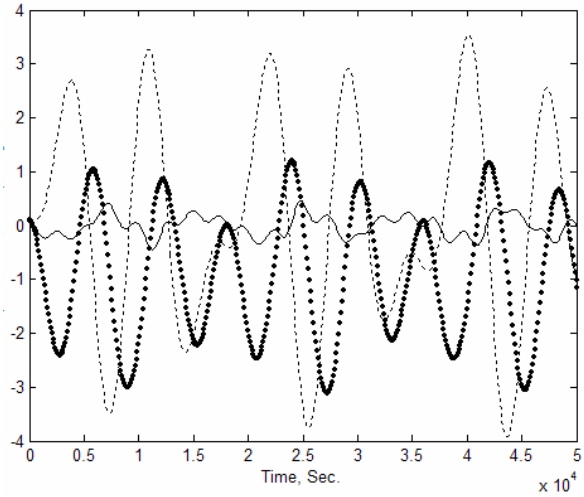

Fig. 14. Attitude response, e = 0.1, I_x = 40, I_y =60, I_z =120 and I_{yz}/I_{tot} = 10/220. yaw …… , roll _____ , pitch - - - - - -.

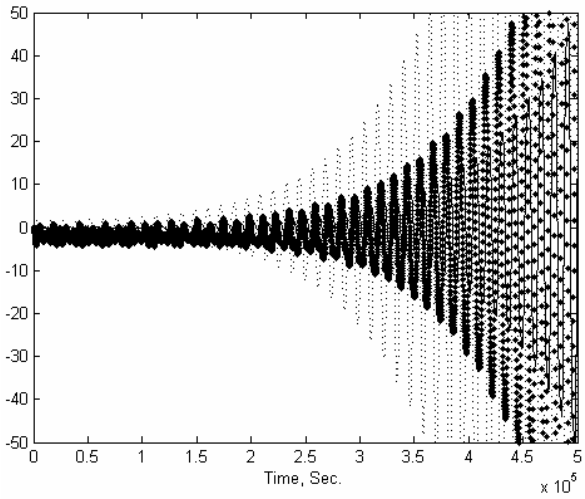

Fig. 15. Attitude response, e = 0.1, I_x = 40, I_y =60, I_z =120 and I_{yz}/I_{tot} = 20/220. yaw …… , roll _____ , pitch - - - - - -.

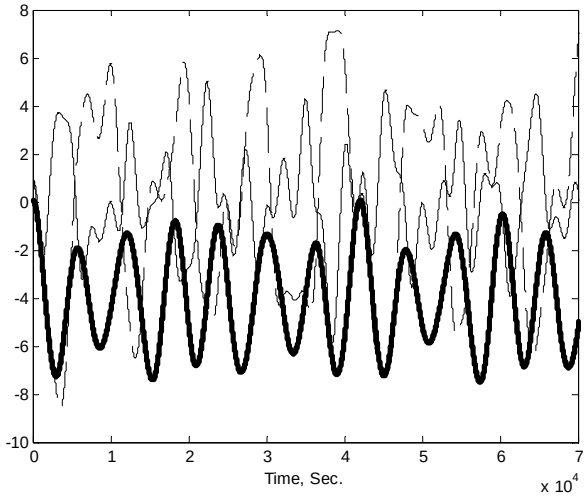

Fig. 16. Attitude response, e = 0.1, I_x = 10, I_y =20, I_z =30 and I_{yz}/I_{tot} = 7/60. yaw …… , roll _____ , pitch - - - - - -.

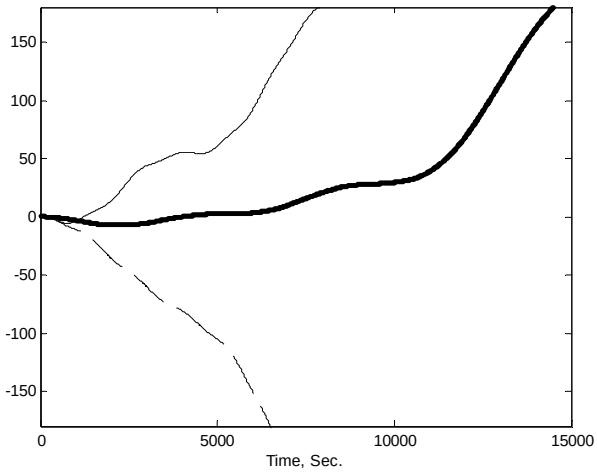

Fig. 17. Attitude response, e = 0.1, I_x = 10, I_y =20, I_z =30 and I_{yz}/I_{tot} = 17/60. yaw …… , roll _____ , pitch - - - - - -.

Closing Remarks

The influence of the mass properties of a satellite and specifically the product of inertia terms, on the attitude dynamics of a rigid satellite subjected to gravity gradient torque, is investigated. It is shown that the classical stable solution of the gravity gradient disturbance, assuming principle moment of inertia with the minimum inertia axis aligned along the local vertical, can become unstable if at least one product of inertia term exceeds a critical value. Stability charts, based on dimensional analysis technique, are developed to predict the long-term behavior of the satellite attitude when the products of inertia terms are present. Numerical test results to verify the developed stability charts showed very successful prediction. These charts can be utilized during the preliminary design stage of the spacecraft to investigate its passive satiability behavior for a given set of product of inertia terms. Furthermore, the influence of the eccentricity of the orbit is that the disturbing effect is more pronounced due to the presence of periodic forcing terms and hence would produce large response for the roll, yaw and pitch if resonance condition prevails.

References

[1] Chen, Y. and Changand, Lin. "Aerodynamic and Gravity Gradient Stabilisation for Micorsatellites." *Acta Astronautica,* 46, No. 7 (2000), 491-499.

[2] Ravindran, R. and Hughes, P.C. "Optimal Aerodynamic Attitude Stabilization of Near-earth Satellite." *J. Spacecraft*, 9, No. 7 (1972), 499-506.

[3] Zanardi, M. and Real, F. "Environmental Torques Acting on a Low Earth Orbiter Cylindrical Spacecraft." *Adv. Space Res.,* 31, No. 8 (2003), 1981-1986.

[4] Roach, R. "Effects of Orbit Ellipticity on Spacecraft Flexible Motion." *Am. Inst. Earon. & Astr.*, Annual Meeting & Tech. Display, 5th Philadelphia, AIAA-1968-1118.

[5] Frik, M. "Attitude Stability of Satellite Subjected to Gravity Gradient and Aerodynamic Torques." *AIAA Journal*, 8, No. 10 (1970), 1780-1785.

[6] Flanagan, R. and Rangarajan, R. "Liapunov Stability Analysis and Attitude Response of a Passively Stabilized Space System." *Acta Astronautica*, 18 (1973), 21-34.

[7] Ashneberg, J. and Lorenzini, E. "Active Gravity Gradient Stabilization of Satellite in Elliptic Orbits." *Acta Astronautica*, 45, No. 10 (1999), 619-627.

[8] Shrivastava, S. and Modi, V. "Satellite Attitude Dynamics and Control in the Presence of Environmental Torques: A Brief Survey." *J. Guidance*, 6, No. 6 (1983), 461-470.

[9] Kaplan, M. *Modern Spacecraft Dynamics and Control*. New York: John Wiley & Sons, Inc., 1976.

تأثير تدرج قوة الجاذبية على القمر الاصطناعي في مدار بيضاوي منخفض وبخواص كتلة غير متماثلة

خالد بن عبداللطيف السيف* و خالد بن عبدالرحمن الدكان**

** قسم الهندسة الميكانيكية، جامعة الملك سعود؛ ومعهد بحوث الفضاء، مدينة الملك عبدالعزيز للعلوم والتقنية، الرياض، المملكة العربية السعودية*

*** معهد بحوث الفضاء، مدينة الملك عبدالعزيز للعلوم والتقنية، الرياض، المملكة العربية السعودية*

(قدِّم للنشر في ٢٠٠٥/٠٣/١٥م؛ وقبل للنشر في ٢٠٠٥/٠٧/٠٣م)

ملخص البحث. يعرض هذا البحث دراسة السلوك الديناميكي لقمر اصطناعي منخفض المدار تحت تأثير تشويشات تدرج قوة الجاذبية عند أخذ حدود عزم القصور الذاتي المختلط وبيضاوية المدار في الاعتبار، فقد ثبت أن الحل التقليدي المستقر لتأثير تشويش تدرج قوة الجاذبية يصبح غير مستقر في حالة تجاوز واحد على الأقل من عناصر عزم القصور الذاتي المختلط قيمة حرجة. وقد تم استخدام طريقة تحليل الوحدات لتكوين مجموعات بدون وحدات بغرض إيجاد علاقة ارتباط بين النتائج المستقاة من الاستجابة الديناميكية لزوايا الدوران المقترنة للمحاور الثلاثة الرئيسية. وبناء على هذه المجموعات تم تطوير خرائط استقرارية للتنبؤ بتأثير حدود عزم القصور الذاتي المختلط على السلوك الديناميكي طويل الأجل للقمر الاصطناعي، كما تم التحقق من هذه الخرائط بالتجارب العددية، حيث نجحت تلك التجارب في التنبؤ بحالة استقرارية القمر الاصطناعي تحت تأثير تشويش تدرج قوة الجاذبية.